

Final Technical Report

Mid to Late Holocene Rupture History of the
Rose Canyon Fault in San Diego, California

Prof. Thomas Rockwell & Drake Singleton
Department of Geological Sciences
San Diego State University
5500 Campanile Dr.
San Diego, CA 92182-1020
P: (619) 594-4441, trockwell@sdsu.edu

Monte and Diane Murbach
Murbach Geotech
3130 N Evergreen Street
San Diego, CA 92110

Award Number G16AP00015

April, 2018

Abstract

We present the results of new paleoseismic trenches excavated across the main trace of the Rose Canyon fault (RCF) in Old Town, San Diego, to determine the timing of late Holocene earthquakes. The stratigraphy at the site consists of historical fluvial and alluvial fan deposits, several buried soil A horizons, massive silt strata, and older San Diego River gravelly secondary channel deposits of Holocene age, and Pleistocene fluvial deposits that likely date to the last interglacial. There is evidence for four large surface-rupturing events, as well as two smaller events, the youngest of which cuts the early historical living surface that contains glass, ceramics, cow bones, and a historical era foundation. This event is likely related to the 1862 San Diego earthquake, which had an estimated magnitude close to M6 and was described as “The day of terror in San Diego” in *The Los Angeles Star*. The possibility exists that additional smaller displacement events have occurred on the RCF, but the stratigraphy at Old Town limits the resolution needed to distinguish evidence for every small surface rupture or cracking event. The four larger events produced substantially more deformation, and over a broader width of the fault zone, than the 1862 event: these events appear as displaced soil horizons, rotated silt beds, offset channel deposits, and fissures filled with overlying sediments. The youngest of these is immediately below the historical horizon and likely correlates with the most recent event recognized at multiple trench sites along the Rose Canyon fault in San Diego and dates to the past 400 years. The three older events have all occurred in the past 3,300 years, with the penultimate large event dated to about 1300 AD. The results of this paleoseismic study, combined with earlier results, indicate that the Rose Canyon Fault has sustained activity throughout the late Holocene and into the Historical period. Comparison of paleoseismic results from the Newport-Inglewood fault (NIF) indicates that some RCF earthquakes have similar timing with NIF events, most likely indicating the occurrence of a sequence or cluster of events on the coastal system of strike-slip faults. The alternative explanation – very large earthquakes rupturing both faults simultaneously – is unlikely when both the slip rate and recurrence intervals for these faults are considered.

Introduction

The Rose Canyon fault zone in San Diego, California follows the broader northwest-striking right-lateral strike-slip motion that characterizes much of southern California’s seismic landscape (Figure 1) (Kennedy, 1975; Sahakian et al., 2017; Rockwell et al., 2016). Recent high-resolution marine seismic imaging (Sahakian et al., 2017) has shown that the Newport-Inglewood fault zone (NIFZ) and the Rose Canyon fault zone (RCFZ), long speculated of connectivity, are indeed one continuous fault system composed of four offshore fault segments connected through structural step-overs, none of which exceeds 2 km in width (Moore, 1972; Sahakian et al., 2017). Thus, the Rose Canyon fault (RCF) is interpreted as the southern onshore expression of the larger Newport-Inglewood-Rose Canyon fault system (NIRC). The NIRC stretches south from its northernmost extent in the Los Angeles basin near Beverly Hills, trending offshore at Newport Bay to cross the continental shelf adjacent to Orange and San Diego Counties, and terminating in the south in San Diego Bay. In total, the NIRC fault system extends for some 170 kilometers, and runs adjacent to many of southern California’s most heavily populated coastal communities. While faults to the east of the NIRC fault,

such as the San Andreas, San Jacinto, and Elsinore faults, have understandably received more attention in both academic circles and public concern because of their direct effect to onshore infrastructure and high seismic hazard, recent research has demonstrated that

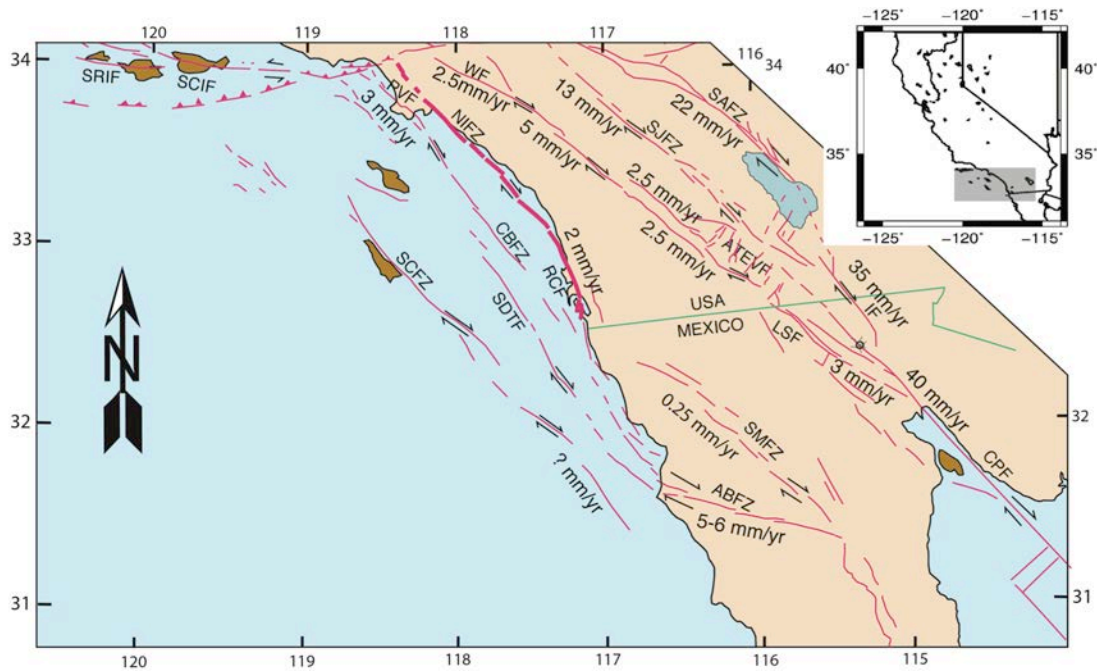


Figure 1. Active faults of southern California with their corresponding slip rates. Shaded box in inset shows location in California. The trace of the Newport-Inglewood-Rose Canyon Fault system is bolded. SAFZ=San Andreas fault zone, IF=Imperial fault, SJFZ=San Jacinto fault zone, EFZ=Elsinore fault zone, CPF=Cerro Prieto fault, LSF=Laguna Salada fault zone, SMFZ=San Miguel fault zone, ABFZ=Agua Blanca fault zone, RCF=Rose Canyon fault zone, NIFZ=Newport Inglewood fault zone, CBFZ=Coronado Bank fault zone, SDTF=San Diego Trough fault, SCFZ=San Clemente fault zone, WF=Whittier fault zone, SCIF=Santa Cruz Island fault, SRIF=Santa Rosa Island fault.

the NIRC represents a significant seismic hazard to much of coastal southern California (Rockwell, 2010a; Sahakian et al., 2017; Leeper et al., 2017), indicating the need for additional studies on the earthquake history of the RCF in San Diego.

The RCF has experienced about four kilometers of right lateral slip based on offset of the Eocene Mt. Soledad conglomerate (Kies, 1982). The timing of this offset is inferred to be Plio-Quaternary, as the upper portion of the San Diego Formation is a tectono-stratigraphic unit that records the down-dropping and sedimentation in San Diego Bay. The San Diego Formation is estimated to be as old as 3.8-4.2 Ma, based on microfauna content of an exposure on Mt. Soledad (Vanrasco et al., 2012), but part of what is mapped as the upper San Diego Formation contains “Santa Barbara” fauna, which indicates continued subsidence and deposition into the Quaternary (Demere, 1982). The San Diego Formation is capped at many localities by marine terrace deposits of the Linda Vista Sequence (Kern and Rockwell, 1992) suggesting an age of pre-1.5 Ma for the initiation of movement on the RCF.

The primary fault traces and associated geomorphic features in the San Diego region are shown in Figure 2. It is thought that some portion of slip is potentially distributed to the RCF by the Agua Blanca fault system of northern Baja California,

Mexico, of which the Descanso fault is an associated strand (Rockwell, 2010a). South of San Diego, the RCF steps onshore via a releasing right-step from the Descanso fault accomplished through a series of fault segments whose motion partially down-drops San Diego bay (SD Bay) (Moore and Kennedy, 1975; Rockwell, 2010a). North of downtown San Diego, the various fault strands that splay across SD Bay have consolidated into a narrow fault zone. The fault then trends along the I-5 corridor until it makes a restraining bend, resulting in the uplift of Mount Soledad before trending offshore at La Jolla (Kennedy, 1975; Rockwell, 2010a; Rockwell and Murbach, 1999). Throughout its onshore trace, the RCF exhibits predominantly horizontal displacement except in locations where segment obliquity results in oblique motion (Lindvall and Rockwell, 1995).

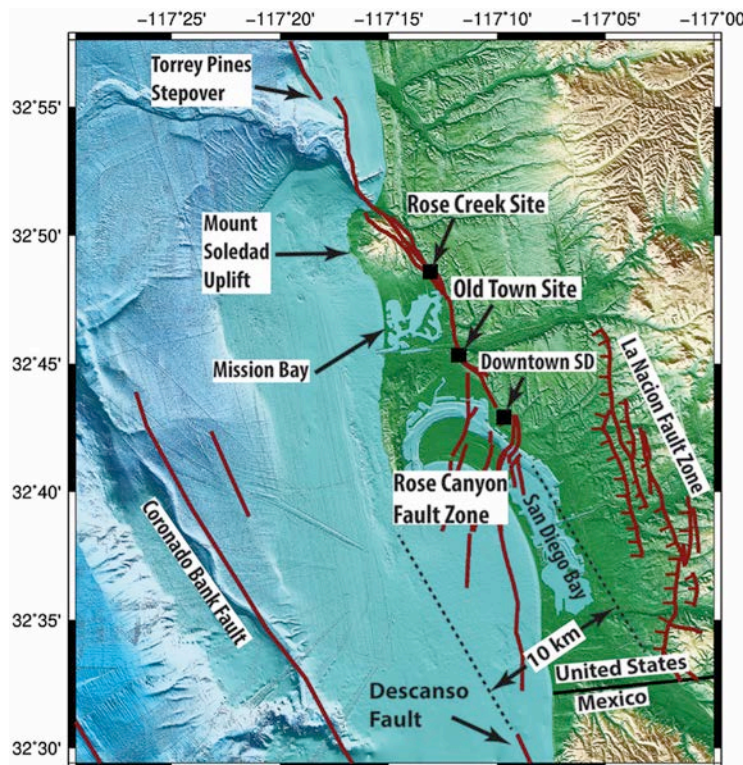


Figure 2. The Rose Canyon Fault zone through San Diego with associated geomorphic expression. From the south, the Rose Canyon Fault zone steps onshore, through San Diego Bay, likely as part of a 10 km stepover from the Descanso fault. Also shown is the La Nacion fault zone, which accommodates minor extension across San Diego Bay (Rockwell, 2010). Locations of the Rose Creek and Old Town paleoseismic sites as well as downtown San Diego are shown as black squares; fault traces

The Rose Canyon fault was first shown to be Holocene active by Rockwell et al., (1991) and Woodward Clyde (1985) whose paleoseismic trenches at Rose Creek and geotechnical survey in downtown San Diego exhibited clearly faulted stratigraphy of Holocene age. Additional 3-D trenching at the Rose Creek site by Lindvall and Rockwell (1995) revealed that the RCF has sustained at least four surface rupturing earthquakes, with possibly more, in the past 11,000 years as well as accumulated a minimum of 8.7 m of lateral displacement in less than the past 8.1 ka, resulting in a minimum slip rate of ~ 1.1 mm/yr throughout the Holocene (Lindvall and Rockwell, 1995; Murbach and Rockwell, 1999) A higher rate of ~ 2 mm/yr was suggested by Rockwell

(2010a) based on deflected stream channels that are inferred to incise the last interglacial marine terrace deposits in Old Town and north of the San Diego River. Of the earthquakes previously documented for the RCF, three events and possibility as many as five, appear to be clustered in time from ~ 9.3 ka to ~ 5.3 ka, after which a period of quiescence of about ~ 5 ka was inferred, based on a moderately developed soil that is developed across several of the early Holocene fault strands at the Rose Creek site

(Rockwell, 2010a; Lindvall and Rockwell, 1995). This “quiet period” was apparently followed by a return to activity with an earthquake displacing the modern topsoil A horizon at Rose Creek, indicating an event date sometime in the past ~400 years (Lindvall and Rockwell, 1995; Rockwell, 2010a). These observations, combined with those from a paleoseismic site in La Jolla and geotechnical surveys in downtown San Diego, support the occurrence of at least one surface rupturing earthquake along this strand of the RCF in the last ~400 years (Rugg et al., 2013; Rockwell and Murbach, 1999; Lindvall and Rockwell, 1995).

However, there was uncertainty as to whether the trenches excavated at the Rose Creek site captured the complete seismic history of the RCF because deposition ceased at the site more than 7 ka BP and there is more than one strand mapped through that area (Lindvall and Rockwell, 1995; Rockwell, 2010a; Rugg et al., 2013). Of particular interest is the apparent absence of any notable earthquakes being documented on the RCF from ~5.3 ka until the most recent event that occurred soon prior to the establishment of the San Diego Mission and Presidio in 1769 AD. The occurrence of surface rupturing earthquakes on the RCF during the mid-to late-Holocene has important implications for the seismic hazard of San Diego and nearby coastal regions, as well as the evolving understanding of southern California’s coastal fault systems. Therefore, a paleoseismic investigation to resolve the discrepancy in earthquake occurrence during the mid- to late-Holocene was warranted. This paper will present results on the earthquake activity of the RCF from two paleoseismic trenches at Old Town in San Diego, California. We present evidence for six earthquake surface ruptures along this segment of the RCF in the past ~3,300 years, and discuss the impact these new findings have on estimates of the recurrence interval for earthquakes along the RCF. We will also discuss possible patterns in the temporal and spatial distribution of reported paleo-earthquakes along southern California’s NIRC fault system, and the possible implications this pattern may have on future seismicity of the Los Angeles Basin.

Methods

Site Selection

Paleoseismic investigations in urban areas are typically very limited due to removal of stratigraphic evidence by mechanical grading and inaccessibility by modern infrastructure. Analysis of historical aerial photography of San Diego from 1927 identified Old Town’s Presidio Hills Golf Course site as an area that has sustained minimal anthropogenic modification, has a high probability of a Holocene sedimentation record, and contained geomorphic indicators of active faulting (Figure 3). In addition, it is inferred that the distributed faulting that is present across SD Bay (Kennedy and Welday, 1980; Kennedy and Clarke 1999) has largely coalesced into a sufficiently narrow zone of faulting just south of Old Town (Rockwell, 2010a) such that a paleoseismic site in Old Town should capture most or all Holocene ruptures.

Trench Investigation

In order to minimize the impact of excavations, two trenches were opened along the boundaries of the Presidio Hills Golf Course. Trench one (T1) was located along the northern boundary of the course, while the second trench (T2) was located along the southern boundary at a slightly higher topographic position in the landscape (Figure 3).

The trenches were excavated by a backhoe and stabilized with hydraulic trench shores. T1 was excavated first from east to west, but contact with a Spanish Colonial era foundational wall at the western-most portion of the trench abruptly halted further excavations by mechanical equipment before the main fault trace could be encountered. The trench did expose a secondary strand of the fault, and the trench was deepened by hand across this fault. A trench-wall grid of half-meter by half-meter spacing was emplaced for a reference frame. Etching of some contacts and fault strands was done because of the poor light conditions for photography, as well as the generally similar color of the stratigraphic units. Two trench mosaics were constructed of the south wall, one photographed under natural light and a second with a halogen light source, as the

trenching was done in late November when light conditions were poor. The northern trench face was only photographed once.

The photomosaics were used as the base for logging, which was conducted in the field. Following the logging and backfilling of the T1 excavation, a second trench, T2 was initiated along the southern margin of the golf course. A one-meter by half-meter grid was emplaced on the southern trench face for the entire length of the trench, and on the northern trench face across the fault zone, both of which were photographed to construct a mosaic for logging. The weakly to massively bedded silt stratigraphy at this location required significant hand etching of all contacts and faulted surfaces so that they would be easily identifiable on the photomosaics of the trench faces, as the stratigraphy was general the same color and dark, and light conditions in December and January were generally poor.

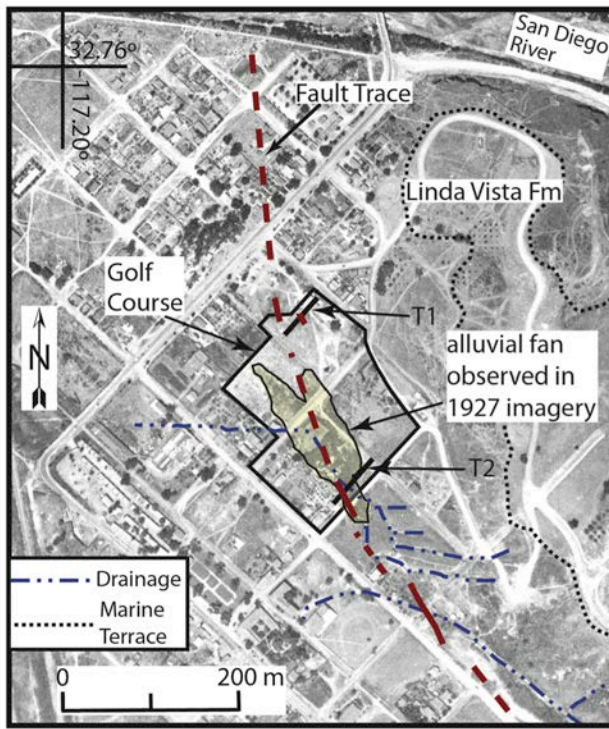


Figure 3. Aerial photograph from 1927 showing the trace of the Rose Canyon Fault through the Old Town area. The location of the future Presidio Hills Golf Course is outlined along with the two trench locations. The alluvial drainages and alluvial fan seen in the exposures of trench T2 are also shown. Note the right-lateral deflection of the drainages indicating active motion of the Rose Canyon fault through Old Town.

Radiocarbon Dating

Detrital charcoal was collected for radiocarbon dating, and sample locations on trench walls were flagged, logged, and photographed. In the lab, samples were washed with deionized water, separated from sediments, dried, weighed, and inspected under a microscope. Sample analysis by Accelerated Mass Spectrometry (AMS) was done at the University of California Irvine's Keck Carbon Cycle Laboratory. The ^{14}C dates were

then entered into OxCal v4.3.2 (Bronk Ramsey, 2009; Reimer et al., 2013) to construct a time versus depth profile of sedimentary units, which would be later used to constrain the ages of interpreted paleoearthquakes.

Results

Stratigraphy

The stratigraphy observed in both trenches is consistent with a predominantly fluvial flood plain environment of the nearby San Diego River (Figure 3), with some additional alluvial fan deposits in trench T2 from a nearby small canyon. The separation in trench locations results in a slightly different stratigraphic expression in the trenches, as trench 1 is topographically lower and closer to the river. Common to both trenches are packages of fine- to coarse-grained light-colored sand, massive bedded sandy-silt sections, and several buried soil A horizons which we use to help correlate stratigraphy between the two trenches.

Trench 1

As a result of T1's lower elevation position on the San Diego River flood plain, the natural stratigraphy seen in the trench exposures consisted of stratified sand, sandy-silt, and clayey-silt deposits that are interpreted as primarily the result of overbank sedimentation. Above the natural deposits lie approximately 2 meters of mechanical fill apparently emplaced during the grading and construction of the golf course.

The upper mechanical fill section is divided into three subsections. Unit 1, the top most 30 cm, is an organically-enriched, dark sandy-silt containing abundant shell fragments and scattered brick fragments that we interpret as reworked A horizon and Native American midden deposits. Both an abrupt lower contact and numerous broken shells indicate a mechanical fill origin, likely from a local source. Below unit 1, unit 2a is a meter-thick dense, reddish brown layer of cobbles with clay films and an abrupt upper and lower contact, likely derived from either the San Diego or Linda Vista Formations. The clay films are interpreted to be inherited from the soil developed in the source deposit. Scattered among the cobbles are brick fragments demonstrating its' artificial fill origin. The base sequence of unit 2, unit 2b, is composed of dark, fine-grained sandy-silt and clay that is organic rich and dense, indicating mechanical compaction. A partial ear of an earthenware urn handle (or a similar cooking artifact) was recovered from within this stratum, indicating a historical age. Unit 2b also contained localized clusters of angular blocks of B horizon material (oxidized, clay-enriched) and the upper portion buries a Spanish or Mexican era Foundation structure. Unit 2b is interpreted to be the result of locally, redistributed topsoil mixed during grading of the golf course, whereas the upper unit 2a was likely brought in from an outside source to raise the northeastern corner of the golf course up to a desired grade level. Hence, we use unit 2b as an historical living surface to correlate to the stratigraphy in trench T2.

Unit 3 and 4 comprise natural strata of T1 and are exposed for the length of the trench, however unit 4 is mostly exposed in the hand-excavated portion of the trench, which was excavated down below the original base of T1. Both units show evidence of multiple flooding events so that further subdivisions were warranted. Unit 3a is composed of light brown, clean (well-sorted) sand, about 30 cm thick, and is interpreted as the result of overbank sedimentation from the adjacent San Diego River. The top of

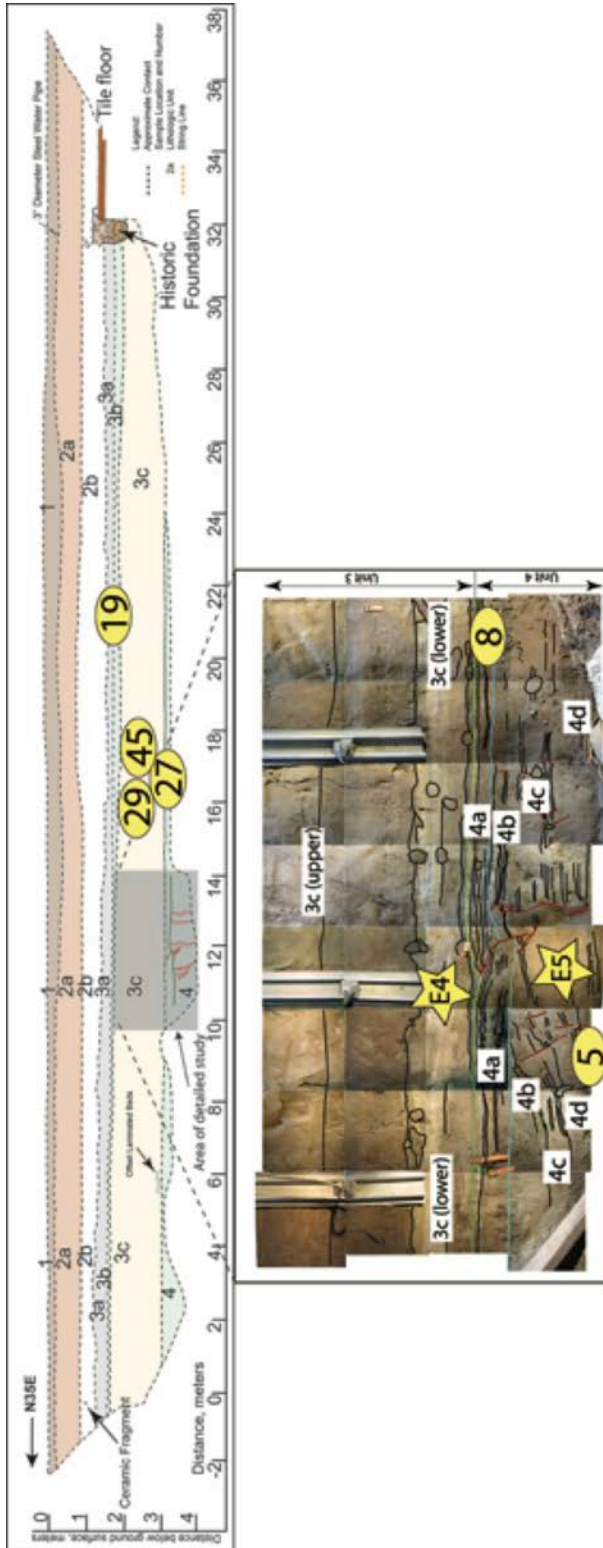


Figure 4. Log of south face of trench T1 with photomosaic of hand excavated section showing faulted stratigraphy.

unit 3a lacks any kind of a developed A horizon and is seen to pond against or bury the Spanish era foundation wall, although it is likely that unit 2b is the disturbed A horizon for this stratum. Together these observations suggest a very young historical age for unit 3a and a single radiocarbon sample collected from unit 3a confirms an age younger than AD 1660. Construction of the Derby Dike (to protect Old Town from flooding) limits the likely upper age bound to 1853 (Abbott, 1991).

Unit 3b is of clear alluvial origin and is characterized by stiff, dark brown sandy silt with minor clay. The top of unit 3b is likely a buried A horizon which represents the early historical living surface prior to flooding and deposition of unit 3a. (Note, both the buried A horizon at the top of unit 3b and the redistributed A horizon of 2a may represent historical living surfaces, with historical sedimentation at trench T1 separating the two. Trench T2, as discussed below, exposed only a single historical living surface, which collectively correlates to these two.) Unit 3c is a 1.3 m thick section of sand, which based on the presence of several buried weakly-formed A horizons, likely represents multiple flooding events. Unit 3c is further subdivided based on the best developed A horizon. The lower unit 3c is composed of clean, well-stratified cross-bedded sand with sparse krotovina, while the upper part of unit 3c is massive, organic-rich, dark brown, silty-sand with many krotovina and has at least one, but possibly two, buried A horizons. Together these two subunits are interpreted to represent at least two

flooding events, with a depositional hiatus when the soil A horizons formed. The Spanish era foundational wall appears to have been excavated into units 3b and 3c suggesting that unit 3b was the historical ground surface at that time. Unit 3a is therefore best interpreted as a historical flood deposit capped by another A horizon.

Unit 4 is subdivided into four subunits based on stratigraphic and structural factors, and is the stratum that contains all evidence for faulting in T1. Generally, unit 4 is a sequence of stratified silty-clay, clayey-silt, sandy-silt, and muddy-sand with abundant krotovina that is interpreted as a result of overbank sedimentation on the San Diego River floodplain. When not obscured by bioturbation, individual strata can be traced for several meters. The stratigraphy is relatively better preserved on the south face of the trench, especially near the faulted surfaces; on the north face the stratigraphy is more massive making interpretations more difficult.

Trench 2

The stratigraphy exposed in T2 has a predominantly alluvial characteristic that can be divided into three distinct alluvial sections: 1) well-bedded, oxidized gravelly sand strata loaded with historical debris interpreted as post-1850 alluvial fan and fluvial deposits; 2) bedded to massive clayey and sandy silt deposits with some gravelly sand or sandy gravel deposits interpreted to be Holocene alluvial fan and fluvial deposits; and 3) an older silty and sandy gravel deposit with a well-developed clay-enriched soil interpreted to be Pleistocene alluvial deposits. Each is discussed in more detail below.

The topmost meter to half-meter of T2 exposed predominantly coarse- to medium- to fine-grained oxidized sandy strata. Units 30-60 are composed of sub-rounded poorly sorted coarse- to fine-grained yellow to light-brown sand with intermixed clusters of rounded to well-rounded poorly-sorted pebble and cobble clasts with scattered boulders. Abundant historical artifacts such as brick, tile, glass, pottery, and bone were found in-situ within units 30-60. Units 70-95 are composed of coarse- to medium- to fine-grained light brown to reddish-brown sand with localized cross bedding, and clusters of pebble-sized clasts concentrated at the thalwegs of small channels. Scattered fragments of historical artifacts, such as brick and iron bars, were observed in units 70-95. Together these units make up several small alluvial channels that have locally eroded into the underlying strata, unit 100. We interpret these units to represent deposition from the alluvial drainage immediately to the south, and onto the alluvial fan seen in historical imagery (Figure 3).

A section of Holocene aged deposits lies directly below an erosional to depositional contact at the base of the historical-aged sand and gravel. The Holocene section, the age of which is based on numerous radiocarbon dates as discussed below, consists of massively bedded brown to dark-brown sandy-silt units bedded with several alluvial channel deposits composed of well-rounded poorly-sorted pebble- to cobble-sized clasts supported by a coarse-grained sand matrix. Several buried A horizons can be recognized in this section, implying periods of non-deposition and surface stability. The relatively massive nature of part of this section is apparently due to bioturbation associated with the periods of non-deposition, as several distinct, thinly bedded silt strata are locally obscured by krotovina (filled burrows), and other parts of the section display obvious filled burrows.

The Holocene-aged deposits are capped by unit 100, a 10-15 cm thick stiff brown

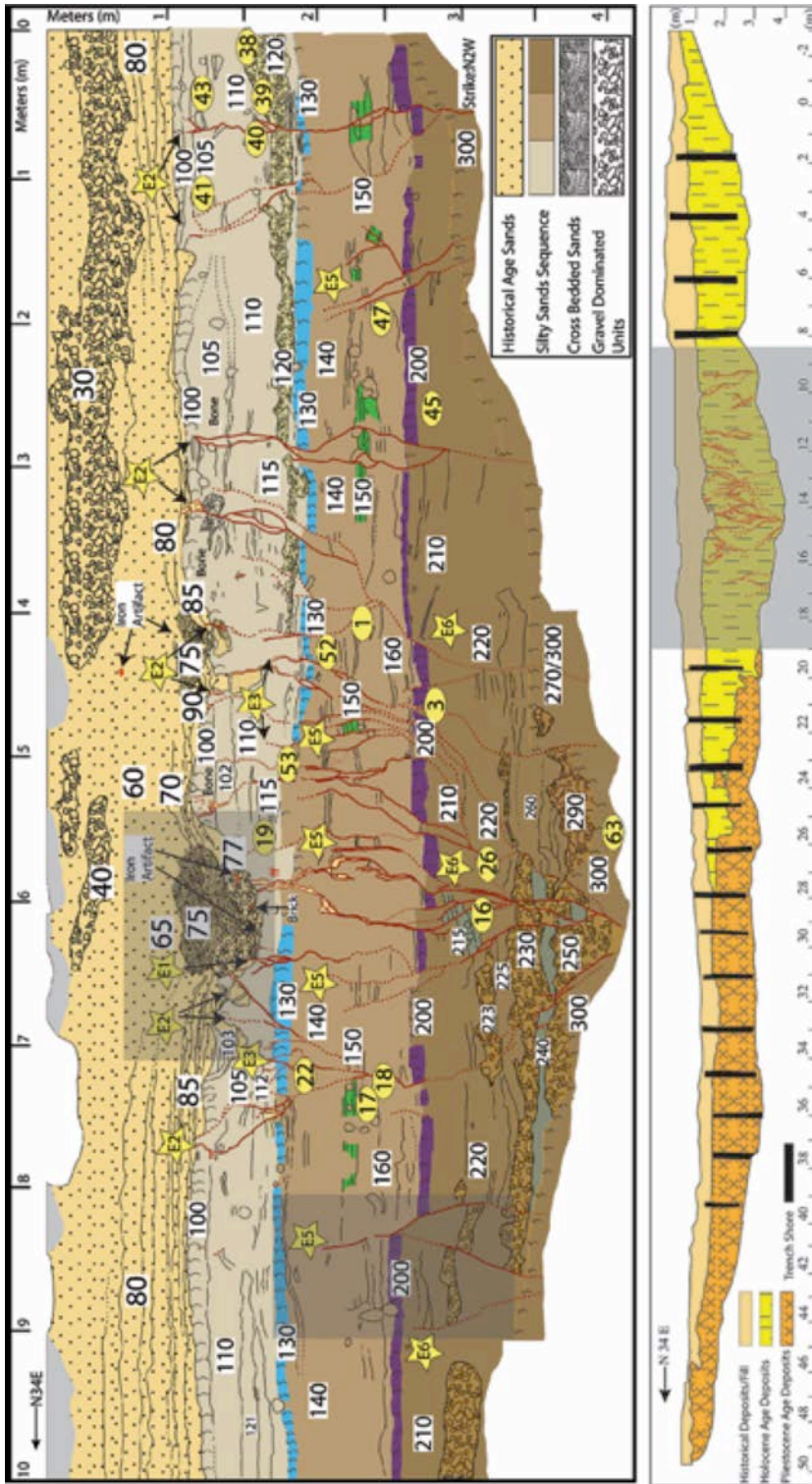


Figure 5. 5a) Top figure shows log of trench T2 south face. Locations of interpreted event horizons are marked as gold stars. Locations where detrital charcoal was sampled for radiocarbon dating are marked as yellow ovals. Stratigraphic units are marked with white boxes. Shaded areas correspond to detailed close ups shown in figures 9 and 10. 5b) Bottom figure shows log of full south face. Shaded area is the location of figure 5a.

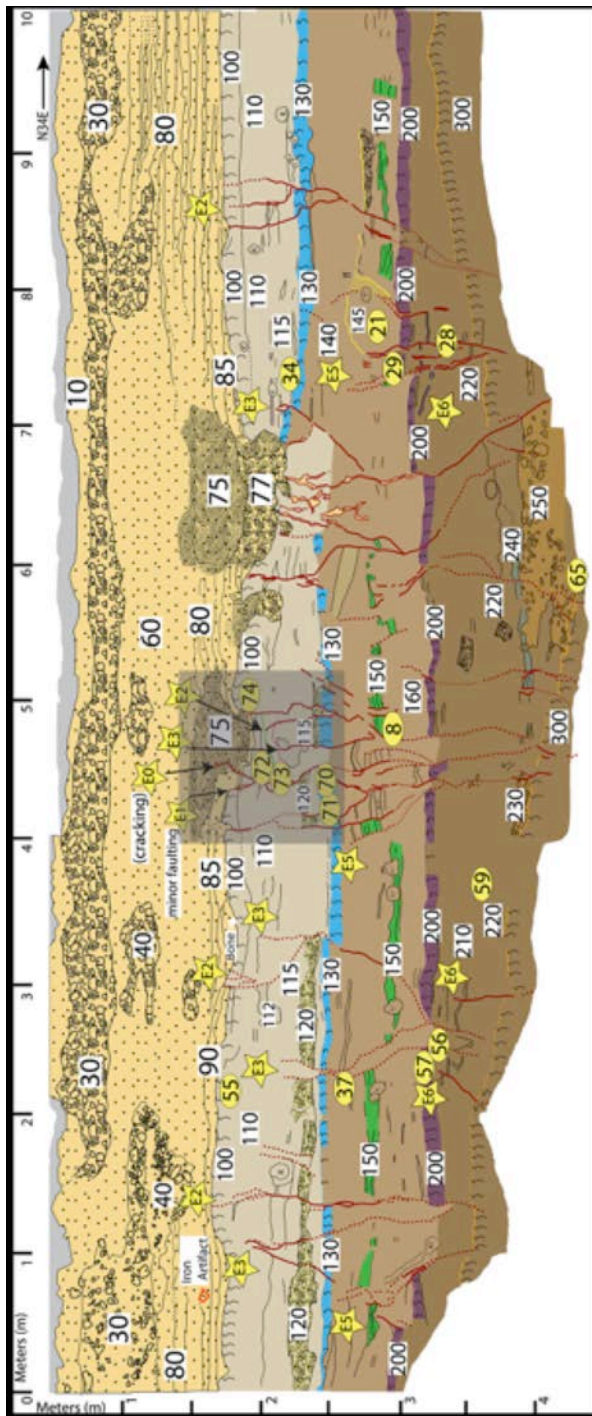


Figure 6. Log of trench T2 north face. Locations of interpreted event horizons are marked as gold stars. Locations where detrital charcoal was sampled for radiocarbon dating are marked as yellow ovals. Stratigraphic units are marked with white boxes. Shaded areas correspond to detailed close up shown in figure 8.

fine-grained silty sand interpreted as a buried A horizon that has been heavily bioturbated, and has been faulted by the main fault strand as well as several auxiliary strands. The upper most section of unit 100 hosted rare bone and glass fragments, as well as evidence for burn pits filled with cow bone excavated into the stratum. Based on the clean contact with the overlying historical alluvial sands, except where the largest alluvial drainages have eroded into and below unit 100, as well as the inclusion of anthropogenic artifacts, we interpret unit 100 to represent the living surface at the time of Old Town's founding sometime after 1769 AD. This surface and A horizon likely correlate to either or both unit 2b (redistributed A horizon) and the A horizon that caps unit 3b in trench T1.

Below unit 100 is a half-meter sequence of brown to dark brown sandy silt strata, Units 110 and 115, at the base of which is a gravelly channel deposit, unit 120, composed of pebble to gravel clasts supported by a light-brown fine-grained sandy-silt matrix. Unit 120 is clearly expressed in the westernmost portion of the trench and progressively thins eastward towards the fault zone.

Unit 130 is a dark brown, fine-grained sandy silt stratum interpreted as another buried A horizon. Unit 130 can be traced relatively well for the length of the trench through the faulted section, and exhibits a small northeast up component of vertical separation across the fault. Below unit 130 and within another sequence of massively bedded, brown sandy silt sediments (units 140-160) is a relatively well-expressed package of thinly bedded strata mapped as unit 150, which is

composed of several yellow to light-brown sand and silt layers that are preserved sporadically for the length of the fault study area.

Unit 200, based on its darkened color is interpreted as another buried A horizon that caps a lower sequence of sandy-silt beds, units 205-220, and was again identified by the dark coloration, porosity, its massive, fine grained texture, and by its abrupt upper contact.

Units 225 through 290 were exposed in the deepest portion of the trench, ~1.5 meters directly below the deepest portion of the historical alluvial channel, and are composed of poorly-sorted rounded clasts, pebble to cobble in size, with intermixed fine-grained sandy-silt strata. Finally, unit 300 lies at the base of the trench and is interpreted as a possible fourth weakly developed buried A horizon. It crops out at the western and eastern edges of the area of detailed fault zone study, but has been removed towards the center likely by erosion of younger alluvial channels of unit 225-290 (figures 5a and 6).

We interpret the entire section of massively bedded sandy-silt units, units 100-300, to represent deposition by overbank sedimentation from the San Diego River or from the nearby small drainage immediately to the south of T2 (figure 3). The intermixed strata that support large clasts, such as units 120 and 225-290, are interpreted to be the result of alluvial channel deposition from the small drainage because they trend towards the San Diego River, parallel to the trend of the small drainage and slope of the alluvial fan, as observed in early photography. In contrast, the well-defined silty strata of unit 150 are likely to be the result of San Diego River overbank deposition as they are sub-horizontal where not disrupted by faulting and laterally continuous where not disrupted by bioturbation.

East of the fault-zone, the Holocene deposits erode into and buttress against the older, Pleistocene deposits (Figure 5b). The older deposits exposed towards the eastern half of the trench are interpreted to be Pleistocene in age because they express a reddish argillic (Bt) horizon developed into the upper part of the soil profile and contain a secondary calcium carbonate (Bk horizon) in the lower part below the argillic horizon. These deposits likely date to the last interglacial period (MIS 5), as post-stage 5 climate in coastal southern California is known to have been wetter and cooler than present (Heusser, 1978), and no late Pleistocene San Diego area soils that post-date stage 5 contain secondary carbonate. Because the fault does not cut these deposits, they are not described further.

Overall, we interpreted the stratigraphy seen in T2 to be the result of its location higher in elevation on the San Diego River flood plain where intermixing of overbank sediments, auxiliary fluvial channels, and outflow of alluvial drainages occurs. Consequently, confident correlation of strata between trenches T1 and T2 is difficult without confirming age control, as discussed below. Nevertheless, the presence of buried soils indicates that there were periods of non-deposition and surface stability, and combining the presence of these soils with the general characteristics of each section allows for a rough correlation of units. For instance, the “living surface” atop unit 100 in T2 most likely correlates with the pair of buried top soils in T1, represented by units 2b and 3b. Because the unit 2b and 3a strata in T1 bury the early Spanish or Mexican era foundation wall and therefore must be historical in age, and as T1 is lower and closer to the San Diego River, it makes sense that the T1 site would sustain more frequent flooding, resulting in an extra depositional unit that is not observed in T2.

Similarly, unit 3c appears to be a major flood deposit associated with flooding of the San Diego River, and as it contains at least one weakly-formed buried A horizon, it must represent more than one flood event separated by some time, probably years, in order to form a weak soil. As flooding of the San Diego River can only be attributed to a major rainfall event, and this unit is stratigraphically below the historical living surface, we tentatively correlate at least one of these flood events with the gravel of unit 120 in T2, which also must represent a major rainfall event and associated flooding from the side canyon.

Marine shells of almost certain Native American origin were found laying on top of unit 4, indicating that the top of unit 4 was a ground surface for at least a short period of time, although there is only very weak soil development based on darkening of the top of unit 4a. Similarly, the top of unit 4b is abrupt but lacks any recognizable soil development. Considering that these strata are thinly bedded in T1 and although locally bioturbated, they retain the finely bedded characteristics of repeated overbank sedimentation, they likely represent an environment that was too wet for occupation by burrowing animals most of the time. In contrast, correlative stratigraphy in T2 are higher on the flood plain and may exhibit more A horizon soil development because floods more rarely reach to the topographic level of T2. Using this line of thought, we tentatively correlate the strata of unit 4 to the more massively bedded fine-grained sediments of units 125 through 160.

Age Dating of Units

Sediment ages were determined through radiocarbon analysis of detrital charcoal collected in situ. Age determination of sediments using detrital charcoal is limited in temporal accuracy by the effects of carbon inheritance during growth, death, initial burn and subsequent transport to the depositional location. This inheritance can be compensated for, to a degree, by the collection and analysis of a large number of samples so that suspected inheritance of one sample can be identified by comparing its age to that of neighboring samples. However, age estimates determined using detrital charcoal will inevitably have some amount of inheritance associated with them and will thus be at least a little older than the actual age of the sediment from which they are collected.

T1

In T1, the detrital charcoal samples that were dated came primarily from the hand-excavated section. Beginning towards the top of the natural section, sample # 19 was collected from unit 3a and yielded a calibrated date range of 267-291 years before present (yrs BP). No radiocarbon samples were dated from unit 3b, but below in unit 3c three samples (# 27, # 45, # 29) returned a date range of 957-1174 yrs BP. Approximately 4 cm above the base of unit 4a, sample #8 was dated to 1326-1407 yrs BP. Below unit 4a, sample #12 was collected ~4 cm above the contact between units 4c and 4b and was dated to 1377-1519 yrs BP. Two samples were collected from unit 4c, #13 and #35, returning a date range of 1566-1855 yrs BP. Lastly, sample #5 was collected ~7 cm from the base of the trench T1, well within unit 4d, and yielded a calibrated radiocarbon date of 2215-2346 yrs BP. These dates were run through OxCal (Bronk Ramsey, 2009), resulting in the age model presented in figure 7.

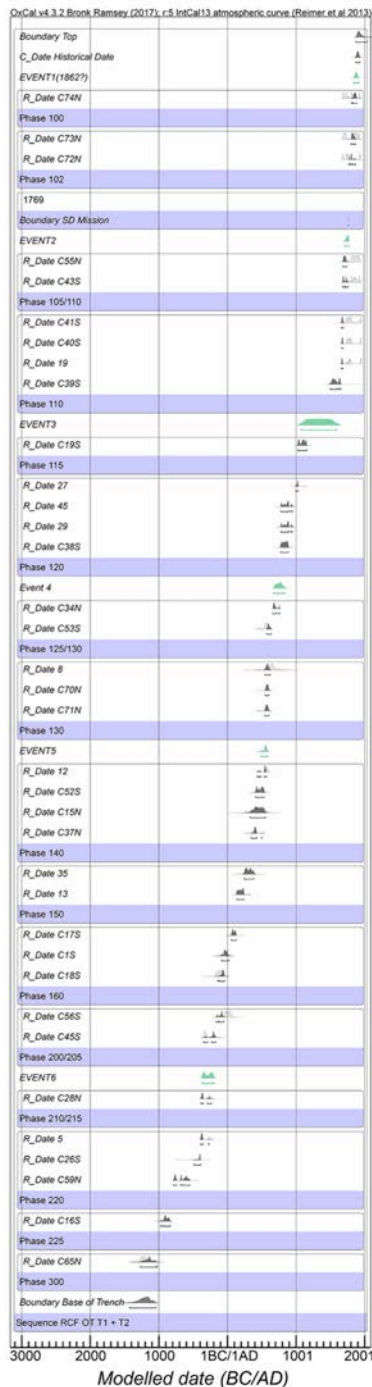


Figure 7: Age model for Old Town developed with dates listed in table T1. Shown are the probability density functions (PDF) for each sample collected in Old Town. Also shown are the event PDF's (shown in green) determined by OxCal. Age model developed through OxCal v 4.3.2 (Bronk Ramsey 2009).

T2

The abundance of historical artifacts found in units 30-90 suggests a historical age decades after first settlement of the Old Mission in 1769 AD. Additionally, the inclusion of scattered fragments of pottery, bone, and brick within the top 1-3 cm of unit 100 suggest that the uppermost portion of this horizon represents the living surface at the time of Old Town's founding and very early settlement. Therefore, we interpret an approximate age of circa ~1800 AD and younger for those units which make up the coarser grained alluvial sands.

From the Holocene age deposits a total of 34 detrital charcoal samples were dated from T2, collected from both the north and south faces. Samples that were collected from units 100-110 returned an age range of 65-455 yrs BP. Above unit 120, sample C14-19S was collected from unit 115 and was dated to 796-925 yrs BP. Sample C14-38S was collected well within unit 120 and yielded a calibrated age of 1065-1173 yrs BP. Below unit 120 and at the contact between unit 130 and the overlying unit 125, two samples returned an age range between 1187-1377 yrs BP, while samples C14-71N and C14-70N returned a date range of 1345-1405 yrs BP for unit 130. Three samples were also collected and dated from unit 140, resulting in a date range of 1396-1616 yrs BP. Above unit 200, three samples were collected from unit 160, which yielded a radiocarbon date range of 1823-2093 yrs BP.

From unit 200 two samples resulted in calibrated ages of 2000-2298 yrs BP. Samples collected throughout units 210 to 225 yielded a calibrated date range of 2341-2923 yrs BP. Finally, at the base of T2 located approximately 2-3 cm below the top of unit 300 sample C14-65N returned a calibrated age of 2974-3216 yrs BP, in good agreement with neighboring samples. As discussed previously, sediments exposed in the eastern portion of the T2 likely date to the Pleistocene based on the presence of the well-developed soil capping the alluvium

and no further dating was attempted for this unit.

Both trenches returned radiocarbon samples that exhibited excellent stratigraphic temporal consistency, with calculated ages generally becoming younger from the base of the trench to the top (figure 7). Seven C14 samples showed evidence for some amount of inheritance and were excluded from the age model (Table 1).

Final Correlation of Stratigraphic units in T1 and T2

The close relative spacing of the two trenches, along with the radiocarbon dates and general similarity in stratigraphic packages, allowed us to more confidently correlate the stratigraphy between the two trenches. While the encountering of the Spanish Colonial Era foundational wall prohibited a full investigation of faulting in T1, it was beneficial as a tie-in point when correlating between the two trenches. Based on the interpretation of unit 2b as redistributed natural topsoil capping unit 3a, the observed floor of Colonial structure at a similar stratigraphic level as the lowest portion of unit 3a (with the upper portion ponding against the foundational wall), and base of the foundational wall excavated into unit 3b, we confirm the interpretation that the upper two sections of unit 3 (3a and 3b) and unit 2b were the historical living surfaces at the time of first historical occupation and in the decades thereafter. A single radiocarbon date from unit 3a in T1 confirms a young age of 1660-1950 AD. The presence of glass, iron bar, and bone found in units 100-110 in T2, as well as radiocarbon dates indicating an age of 1500 - 1892 AD, suggests that these units also represent the historical living surface and shallow (~15 cm) subsurface during the earliest periods of occupation. We therefore confirm the interpretation that units 2b, 3a, and 3b in T1 are time synchronous with units 100-110 in T2.

Continuing down the trench profiles, the silty-sand of unit 115 in T2 can be correlated with upper portion of unit 3c in T1, which is also represented by a massive section of silty-sand. We interpret the clean cross-bedded sands of unit 3c in T1 to represent higher flow during overbank sedimentation, perhaps as a consequence of a more southerly course of the San Diego River through Old Town. This period of higher flow deposition in T1 is expressed in T2 as the gravelly deposit of unit 120 which likely represents aggradation of the drainage to the south of T2. Thus, the similarity in stratigraphy, mostly alluvial sand and gravel, interpreted to represent high flow, suggests that the lower portion of unit 3c in T1, correlates to unit 120 in T2, which is confirmed by the close agreement of radiocarbon ages.

The bedded silty-sand of unit 4 in T1, interpreted to represent overbank sedimentation, correlate well with several of the lower massively bedded silty-sand units of T2. For the following correlations we lean more heavily on the close agreement of radiocarbon dates to assist in correlating these more massively bedded silty sand strata. As mentioned previously, the location of T1 lower in elevation on the San Diego River flood plain, when compared to the location of T2, resulted in slight variations in stratigraphy and thus slight differences between the correlated stratigraphic units, as discussed below. We interpret the bedded gray silty clay and clayey silts of unit 4a in T1 that exhibit some A horizon development to correlate with the buried A horizon of unit 130 in T2, which likely formed during a period of non-deposition at T2 and reduced overbank sedimentation at T1. This correlation is confirmed by several detrital charcoal

Table 1. List of radiocarbon samples collected at Old Town-San Diego, CA. Samples names with X in front were excluded from age model based on inheritance discussed in text.

C14 Sample #	North/South (T1/T2)	Unit	Weight (mg)	14C age (BP)	±
74	North (T2)	100	4.3	135	15
72	North (T2)	102	33	150	15
73	North (T2)	102	24	110	20
43	South (T2)	105/110	181.5	135	15
55	North (T2)	105/110	25.6	105	25
40	South (T2)	110	3.7	180	15
41	South (T2)	110	86.6	180	25
19	South (T1)	3a (~110)		195	15
39	South (T2)	110	2.7	305	25
19	South (T2)	115	8.2	950	20
38	South (T2)	120	4.9	1190	15
27	South (T1)	3c (~120)		1005	15
29	South (T1)	3c (~120)		1165	15
45	South (T1)	3c (~120)		1165	15
53	South (T2)	125/130	25.5	1510	25
34	North (T2)	125/130	3.6	1305	15
8	South (T1)	4a (~130)		1400	70
70	North (T2)	130	15.9	1490	15
71	North (T2)	130	4.5	1505	20
15	North (T2)	140	1.5	1610	70
52	South (T2)	140	8.5	1595	20
37	North (T2)	140	4.2	1645	20
12	North (T1)	4b (~140)		1510	15
35	North (T1)	4c (~150)		1725	30
13	North (T1)	4c (~150)		1815	15
17	South (T2)	160	54.7	1915	15
18	South (T2)	160	5.9	2085	15
1	South (T2)	160	10.3	2035	20
56	South (T2)	200/205	3.7	1995	30
45	South (T2)	200/205	18.7	2175	15
28	North (T2)	210/215	11.1	2265	20
5	South (T1)	4d (~215/220)		2265	15
26	South (T2)	220	25.8	2365	20
59	North (T2)	220	14.5	2520	15
16	South (T2)	225	7.8	2760	20
65	North (T2)	300	4.8	2985	35
X 22	South (T2)	140	32.5	165	20
X 21	North (T2)	145	2.4	3940	20
X 8	North (T2)	150	26	2125	15
X 29	North (T2)	160/200	5.3	2475	20
X 3	South (T2)	200	22.3	3785	20
X 57	North (T2)	200	10	2845	15
X 63	South (T2)	300	14.8	4195	15

samples collected from unit 4a in T1 and unit 130 in T2 which yield very similar dates of 544 to 624 AD and 574 to 763 AD, respectively.

Similarly, the heavily biotubated silty sand of unit 140 in T2 is correlated with the bedded brown clayey silts of unit 4b in T1, both of these units contained agreeable radiocarbon date ranges of 344 to 535 AD and 432 to 573 AD, and are therefore interpreted to represent the same depositional time period. Unit 4c in T1 is composed of a sequence of silty clays and clayey silt with a few distinct brownish clay stringers that can be traced laterally throughout the fault zone, this stratigraphy is similar to the distinctive silty-sand stringers of unit 150 in T2 thus, we interpret the finer grained clay stringers in T1 to be correlated with coarser grained silty-sand deposits in T2. Lastly, we correlate the massive to weakly bedded muddy fine sands of unit 4d at the base of T1 with massive silty sands of unit 210 in T2, which is confirmed by the agreement of radiocarbon dates, which yielded date ranges of 397 to 266 BC and 389 to 235 BC, respectively.

By correlating the stratigraphy in the two trenches in this manner, the independent evidence of paleoearthquakes preserved in the separate trenches can be combined. This increased the overall strength of interpretations by supplementing the full width of the fault zone investigation of T2 with the high stratigraphic resolution of T1 on a secondary splay fault. Additionally, comparing the results from the two trenches acts as a check in our interpretations; events seen in trench T1 can be checked against the timing of independently interpreted events in T2.

Evidence of Earthquakes

From the trench exposures in T1 and T2, there is evidence for six surface ruptures in the past ~3,300 years at Old Town, although they do not appear to have all been the same size. In T1, the exposed part of the fault zone, which constituted a secondary fault strand only, is confined to a couple meter wide zone, but the finer stratigraphic resolution facilitated the identification of two events that are closely spaced in time. In T2, where the entire width of the fault zone could be investigated, the fault zone is broader with faulted stratigraphy seen across a ten-meter wide zone. Dates for paleoearthquakes were determined using the radiocarbon calibration program OxCal v 4.3.2, which employs a Bayesian statistical framework on calibrated radiocarbon ages of the confining sediments to estimate probability density functions of the interpreted event horizons (Bronk Ramsey, 2009; Reimer et al., 2013).

Evidence for the youngest event captured in the trench exposures is event E0, which appears as a thin fissure or crack filled with historical-aged sand into the underlying unit 95, as exposed on the north face of T2 (figure 8). We named this event E0 as it is unknown whether this fracture is the result of fault creep, settlement, or some other mechanism; a non-tectonic cause is plausible. The stratigraphic position of the infilling sediment, 20-25 centimeters above unit 100, suggests an age for this event that is substantially younger than 1769 AD, and likely well after 1850 by which time Old Town was firmly established. Although the historical sediments are fissured, there is no recognizable offset or mismatch of stratigraphy indicating only very minor motion, if any.

Event E1 is expressed as fissure infilling and small scale folding of historical-aged alluvial sands on the south face of T2 (figure 9) as well as a small (2-4 cm) displacement of a clayey-silt unit directly above unit 100, the top of which is the early historical living surface, and fissure infilling on the north face of T2 (figure 8). The evidence for event E1 is concentrated in an area directly above the main fault strand. The faulting of sediments containing abundant anthropogenic artifacts indicate a historical age (post 1769 AD), and as it faults the living surface (top of unit 100) which probably saw occupation for some period of time, this event is probably at least several decades younger than the mission and presidio and likely dates to the Rancho Period (1834-1849) or younger.

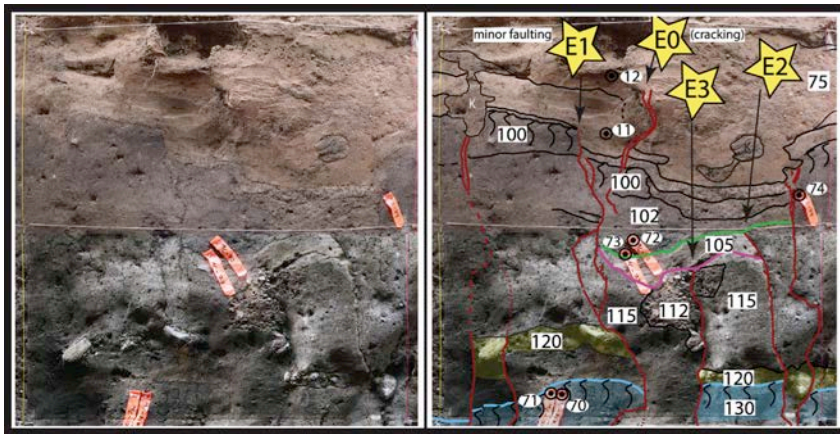


Figure 8. From north face of trench T2 figure shows faulted soil A horizon (Unit 100 and historical living surface at time of California's settlement), buried soil horizon (Unit 105), and fluvial deposits (Unit 112). Panel shows evidence for three separate surface rupturing events as well as minor cracking. Event E3 is seen as faulting to unit 112, event E2 is seen as faulting and fissure infilling of units 105 -100, event E1 is seen as displacement, ~3-5 cm, of historical age alluvial sands. Also shown is fissure infilling of young sediments possibly from triggered slip or creep event.

Evidence for event E2 is expressed over an approximately nine-meter-wide fault zone with stratigraphy generally observed to be faulted up into or through unit 100 and being capped by the alluvial sands of historical age. On the south face of T2 and directly beneath the deepest small alluvial channel incisions, event E2 is seen as fissure infilling of lighter-

colored coarser sediments than the surrounding units. These infilling sediments are derived from the deepest alluvial channels that have eroded into, and well below unit 100 and so lay at a deeper stratigraphic level than the historical sandy strata, which were likely deposited by the historical alluvial fan system seen in historical imagery (figure 3). In sections of the trench away from the small, deep alluvial channels, event E2 is seen as upward terminating fault strands capped by the upper few centimeters of unit 100, as well as tilted alluvial channel deposits (figure 5a and 9). The north face of T2 has similar evidence for event E2 with fissure infilling of overlying lighter-colored sediments, again directly below the same deepest, small alluvial channel, and upward terminating fault strands capped by unit 100 or the historical age alluvial sands (figure 6, 8). Radiocarbon analyses and historical records of seismicity place the occurrence of event E2 between 1708 and 1769 AD, using the timing of Mission establishment as a prior, yielding a mean date of ~1744 AD.

Event E3 is well expressed in T2 and is seen on both trench faces as upward terminating fault strands, capped by unit 110-105 (figures 5a, 6, and 8), as well as fissure infilling to a similar stratigraphic level. The timing of event three is the least well-constrained event date of our study, due to the lack of reliable radiocarbon dates at this

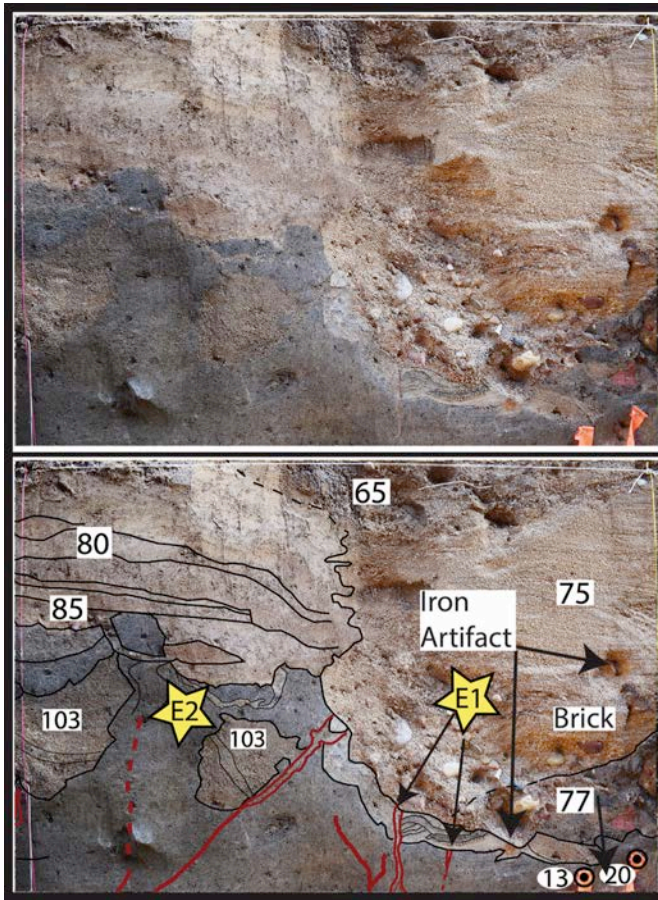


Figure 9. Figure shows evidence for Event E1 and E2 on the south face of trench T2. Event E2 is seen rupturing to unit 100 with tilting of unit 103, a channel pipe composed of medium- to coarse-grained sands. Event E1, interpreted to be the 1862 San Diego earthquake, is seen as infilling of fissure from historical era sands, which contain iron bar and brick.

stratigraphic horizon. As a result, the age of event E3 is best constrained by age of unit 110 above and unit 115 below with a best estimate date range of 1077-1588 AD.

Event E4 is clearly identifiable only in T1 due to the more detailed stratigraphic resolution of T1 when compared to the more massively bedded stratigraphy of T2 for this time period. Event E4 is seen as a single fault strand that offsets the unit 4b/4a contact by about 5 cm, and terminates at the top of unit 4a and is capped by the unfaulted, clean cross-bedded sands of unit 3c (figure 4). Thus, the age of unit 3c provides an upper bound for event E4, while unit 4a provides a lower. This results in a date range of 675 to 835 AD. It should be noted that evidence for event E4 is likely present in T2, but has been amalgamated with event E5 because of the poorer stratigraphic resolution of T2 sediments when compared to T1.

Event E5 is seen at multiple locations on both faces of T2 as well as in T1, although as mentioned above, some of the deformation observed in T2 may be attributable to event E4. On the north and south faces of T2, event E5 is expressed as upward terminating fault strands, all capped by unfaulted sections of unit 130, as well as fissure infilling of overlying sediment. At the eastern- and western-most sections of the south face of T2, event E5 is expressed as ~25-15 cm vertical displacement of unit 200 capped by unfaulted unit 130 (figure 10). In T1 event E5 is expressed as significant faulting and folding of units 4d through 4b, with deformation observed across a ~2-meter-wide zone. This deformation is then planed off and capped by horizontally deposited strata of unit 4a (figure 4). Event E5 is interpreted to have occurred sometime between 486 AD to 588 AD and appears to

be a larger rupture than event E4 based on the associated folding and width of damage zone in T1.

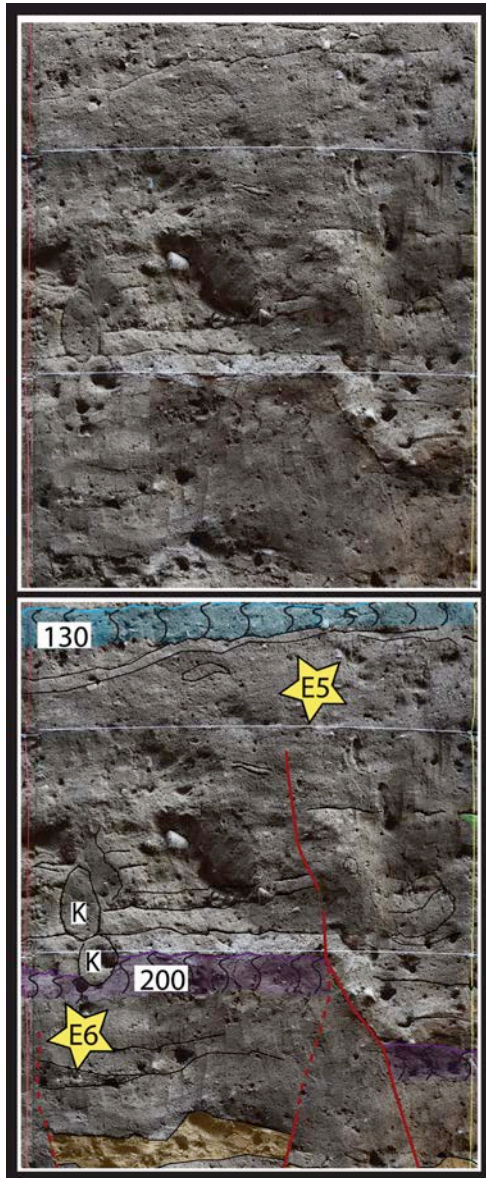


Figure 10. Figure shows evidence for Event E5 and E6 from the south face of trench T2. Evidence for event E6 is seen as upward terminating fault strands capped by unit 200. Evidence for event E5 is seen as vertical displacement (~20 cm) of unit 200 that is then capped by units 140-130.

rills incised into unit 100 and the subsequent deposition of the historical-ages alluvial fan sediments clearly demonstrate that this area has sustained repeated flooding. In any case, we do not attempt to relate this to a specific historical earthquake, although intensity VII was recorded in San Diego from the 1892 Laguna Salada earthquake (Agnew et al., 1979) and is a candidate if the crack is a result of triggering by strong ground shaking.

The oldest event recorded at the Old Town site is event E6 and is observed near the base of trench T2. On the south face, evidence for event E6 includes the tilting and deformation of several fine-grained units including unit 215, which are then capped by the horizontal deposition of unit 200. Additionally, upward terminating fault strands with ~8-12 centimeters of displacement are observed and again capped by unit 200. The stratigraphy at the base of the northern face of T2 is more massive than the southern face and thus does not exhibit the same well-developed auxiliary channel features. However, away from the auxiliary channel deposits we still observe tilted fine-grained silt stringers as well as upward terminating fault strands, all capped by unit 200. Event E6 is interpreted to have occurred sometime between 371 BC to 199 BC. The event ages and their uncertainties are summarized in Figure 11.

Discussion

Earthquake Magnitudes and Late-Holocene Recurrence Interval

The paleoseismic trenches at Old Town show that the RCF has sustained repeated surface rupturing earthquakes throughout the late Holocene and into the Historical period. The extent of deformation associated with each individual event at Old Town can be used to estimate a relative magnitude of the causative earthquake.

Event E0 is a crack with no recognizable offset. Its origin is unclear; it may represent a small component of creep, a small triggered slip event, or it may represent settlement in the fault zone due to percolating surface water, as the presence of several small

Event E1 displaces historical-aged sediments and the top of the unit 100 “living surface” and likely represents displacement from a historical earthquake, probably at least several decades after the arrival of the Spanish in 1769. From the historical records of seismicity there are two earthquakes with reported felt effects more intense, or equal, in San Diego when compared to other locations in southern California: April 12th, 1852, and May 27th, 1862 (Agnew et al., 1979). The event reported in 1852 has a suspect seismic source due to there being only one account of reported damage (on only one structure) (Anderson et al., 1989; Agnew et al., 1979).

Thus, the most likely candidate for event E1 is the May 27th, 1862 AD event, reported as the “Day of Terror in San Diego” by the regional newspaper the Los Angeles Star (*The Los Angeles Star*, 1862; Legg and Agnew, 1979). This event, preliminarily located along the Spanish Bight fault in San Diego Bay or an adjacent fault offshore, is estimated at about M6, which is about the threshold for surface rupture and is consistent with the amount of observed deformation for this event. The reported felt effects of this event, although inconclusive by themselves, when combined with the young surface rupture observed at Old Town support the occurrence of an earthquake on the RCF in 1862 (Legg and Agnew, 1979).

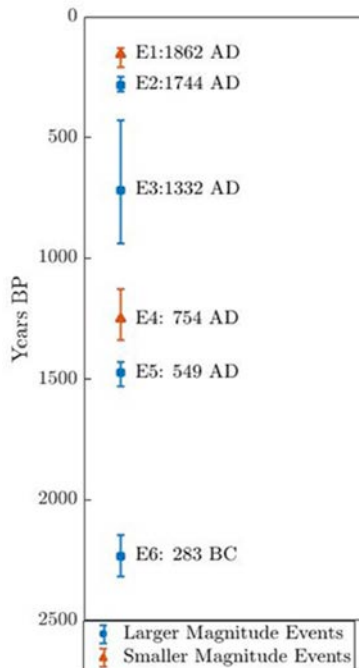


Figure 11. Earthquake dates determined at Old Town site. Error bars are 95% confidence interval.

The penultimate event seen at Old Town, event E2, has caused displacement across the entire fault zone up to but just below the historical living surface, and represents a much broader zone of faulting than seen for E1. Furthermore, E2 correlates well with the most recent event (MRE) reported at other paleoseismic sites in San Diego (Rockwell, 2010a). North of Old Town, at Lindvall and Rockwell’s (1995) Rose Creek site, a cleanly faulted modern topsoil A horizon indicates an event date in the past ~400 years. A young surface rupture for the northern most section of the RCF was confirmed by later work in La Jolla using material, partially derived from a Native American midden, from an infilled fissure to provided a more reliable date of 1650±125 AD (Rockwell and Murbach, 1999). South of Old Town, multiple geotechnical reports in the downtown area have document displacement of the topsoil A horizon as well

as calibrated radiocarbon dates between 1420-1769 AD for the MRE (Woodward and Clyde, 1985 and 1994, as reported in Rockwell and Murbach, 1999). As discussed previously, radiocarbon dates from our Old Town trenches indicate that this event occurred between 1704 and 1769 AD, well within the radiocarbon uncertainty from other sites. Thus, with evidence for event E2 being documented for the length of the onshore segment of the RCF, we infer that event E2 represents a significantly larger earthquake than E1 that ruptured at least from La Jolla to San Diego Bay.

Events E3, E5, and E6 all exhibit similar styles of deformation, e.g., tilted beds, 5-25 cm vertical displacements, and deep fissure infillings over a broad ~10 meter wide zone, similar to that observed for event E2. Based on the similarities in deformation it is likely that events E3, E5, and E6 also ruptured most of, if not all the onshore section of the RCF. Thus, based on the amount of deformation and width of the effected fault zone, we interpret events E2, E3, E5 and E6 all to be the result of relatively larger magnitude earthquakes.

The localized, small vertical displacement (~1-5 cm) associated with event E4 is similar to that observed for event E1 and is therefore also interpreted to be the result of a relatively smaller magnitude earthquake, possibly in the 6-6.4 Mw range. Evidence that it may have been a little larger than the 1862 earthquake is inferred because it ruptured a secondary fault splay in T1 that did not re-rupture in 1862. Hence, the larger inferred magnitude range.

We attribute the difference in observed earthquakes between the two trenches to two factors. First, as mentioned previously the excavation into a culturally significant structure in T1 prevented an investigation of the main fault at that location. We believe the main fault trace is likely located beneath, or slightly west of the Spanish Colonial era structure and was just missed by the mechanical excavations at T1 (Figure 4). As a result additional strands and the primary fault that would have ruptured in past earthquakes were not observed. Second, the higher stratigraphic resolution at T1 enabled us to distinguish event four and event five as separate events despite the close separation in time of approximately 100-200 years. Except for a few select locations, this kind of stratigraphic resolution between closely spaced smaller and larger magnitude events was not possible in trench T2 due to the more massive nature of the silty bedding. Therefore, the possibility exists that evidence for additional, smaller late Holocene earthquakes on the RCF was not recovered at Old Town.

The six earthquakes interpreted at Old Town have important implications for the understanding of the seismic behavior of the Rose Canyon Fault. The period of quiescence previously interpreted to have taken place from ~5.3 ka to ~500 years ago lead Rockwell (2010) to postulate a possible cluster mode behavior for the RCF. However, our results demonstrate that the Rose Canyon Fault has sustained activity throughout the late Holocene, and it would appear into the Historical Period. While there remains a several thousand-year gap in the paleoseismic record of well-dated events, geotechnical reports from the San Diego airport suggest additional earthquakes in the mid-Holocene (Scott et al., 2013). Thus, it would appear that the RCF has ruptured with quasi-periodic frequency for the periods over which a record has been preserved.

Previous estimates of the recurrence interval on the Rose Canyon fault have a broad range of about 3,000 to 800 years, depending on considerations of assumed quasi-periodicity, clustered behavior, and characteristic slip per event (Lindvall and Rockwell, 1995; Rockwell, 2010a). Rockwell (2010a) determined an intercluster recurrence interval of approximately 800 years for the early Holocene events observed at Rose Creek. Using the methods of Biasi et al. (2002), the event dates recovered at Old Town suggest a similar recurrence interval for the inferred larger events of ~ 700 years during the late Holocene. With the suggested mid-Holocene seismic activity at the San Diego Airport, along with the close agreement between the early Holocene recurrence interval of Rockwell (2010a) and that of Old Town, these observations suggest that the Holocene

recurrence interval for the RCF is closer to ~ 700-800 years rather than the 1,000-1,500 years determine from the Rose Creek events alone (Lindvall and Rockwell 1995; Rockwell 2010a, 2010b). However, it is possible that the earthquake sequence seen at Old Town represents the tail end of the most recent cluster, with a shorter quiescence period discussed above. More accurate paleoseismic dating targeting the mid-Holocene will be required to sufficiently resolve this question.

The apparently shorter recurrence interval at Old Town has important implications for slip per event and the average size of earthquakes when combined with slip-rate estimates of the RCF. A previously estimated slip per event of 3 meters implies a slip rate closer to 4.0 mm/yr if the 700-800 year recurrence interval is applied. However, that 3 m estimate for slip in the MRE was based on an offset channel at Rose Creek that may have been offset by two or more events, so was a maximum displacement. An alternative estimate is resolved by using the 700-800 year recurrence interval determined from the early and late Holocene record and applying the 1.5-2 mm/yr slip rate to arrive at an average displacement of 1.2-1.4 m for the larger events and less than a meter for the smaller events. This estimated average displacement is consistent with earthquakes in the M6.7-M7 range.

Effect of Fault Structure on Earthquake Occurrence

The location of Old Town north of the extensional structures that make up the step-over through San Diego Bay may help explain some features of earthquake occurrence at Old Town. The structural setting of San Diego Bay and Old Town is similar to fault structures east of the Peninsula Ranges, where a large releasing step-over is formed by the faults of the Imperial Valley (Elders et al., 1972). A large number of studies have documented triggered slip on faults in the southern San Andreas fault system in the Imperial Valley in response to ruptures on nearby faults (e.g. Wei et al., 2011; Fuis, 1982). This similarity in fault structure and orientation may explain a mechanism for the interpretation that event E0 is potentially the result of either trigger slip or possibly shallow creep; however, a non-tectonic origin should not be ruled out.

If E0 represents a trigger slip event, its event horizon, well within the historically-aged sand strata but prior to construction of the golf course, suggests an event age sometime around the turn of the 20th century. Faults of coastal northern Baja and offshore of San Diego (e.g., the San Miguel-Vallecitos fault and the Agua Blanca fault system) exhibit a spatial distribution and orientation with respect to the RCF similar to that of the Imperial Valley, and so would be the most likely triggering mechanisms for event zero. Alternatively, the February 1892 earthquake on the Laguna Salada fault in northern Baja California was the last earthquake to have produced intensity VII damage in San Diego (Agnew et al., 1979) and is also a plausible triggering mechanism. Further, the area's historical record of seismicity has numerous accounts of earthquakes during this time period that likely occurred on the faults of coastal northern Baja, but without precise dating of the event zero horizon we do not attempt to identify a causative earthquake (Agnew et al., 1979).

For at least two occurrences at Old Town, small magnitude events inferred from minimal displacement on a limited number of fault strands were observed to occur shortly after larger magnitude events that shattered the full width of the fault zone. The event E4 horizon is dated approximately 150 years after that of event E5, while event E1

appears to follow event E2 by about 100 years. Similar behavior has been observed on other faults in southern California, and has been modeled as the result of reduced normal stress on extensional structures following large earthquakes (Stein et al., 1992; Nielsen and Knopoff, 1998). Thus, this pattern is possibly also a result of Old Town's proximity to the large extensional step in the RCF across San Diego Bay, which may allow for the preservation of some "tension aftershocks" described by Nielsen and Knopoff (1998).

The paleoseismic record at Old Town has at least twice, but possibly more given the limitations in stratigraphic resolution of T2 discussed previously, captured the occurrence of a relatively larger magnitude earthquake on the Rose Canyon fault, which is then followed by slip that is possible transferred to the Old Town section of the RCF by one of the linking dip-slip structures that splay across San Diego Bay. It is our interpretation that this scenario likely described the penultimate event E2, which is interpreted as a larger magnitude event that would have relieved the regional stresses in San Diego Bay allowing the initiation of earthquakes on nearby faults, such as the Spanish Bight, at a lower shear stress, resulting in E1.

Cascading Seismicity of the Newport-Inglewood-Rose Canyon Fault System

With the RCF interpreted to represent the southern onshore extension of the larger NIRC fault system, the increased activity in the late Holocene seen at Old Town has important implications for the seismic behavior of the larger NIRC. It has been suggested that the close spacing, in time, of the most recent paleoseismic events along the Agua Blanca fault, RCF, and Newport Beach segment of the NI fault, represents a northward cascading sequence of earthquakes (Grant and Rockwell, 2002). The proposed cascade includes the MRE seen at both Rose Creek and La Jolla, and now Old Town with event E2 occurring sometime in the mid 18th century (Grant and Rockwell, 2002). Recently, new work at Seal Beach has found evidence for three late Holocene earthquakes that are interpreted based on rapid subsidence of a fault bounded marsh along the southern, onshore segment of the NI fault (Leeper et al., 2017). The NIF events appear to correlate well with the events determined at Old Town (Figure 12). Additionally, researchers working at other sites on the NI and the Compton-Los Alamitos blind thrust (CPT-LA), which maybe kinematically linked with the NI at depth, further correlate with the results at Seal Beach, Rose Creek, and Old Town (Grant et al., 2002; Grant et al., 1997; Leeper et al., 2017; Leon et al., 2009; Wright, 1991). The close correlation in time, through multiple earthquake cycles of dated paleoearthquakes along the various segments of the NIRC fault suggests that this fault system does indeed communicate stress between fault segments in either very large earthquakes or a cascading sequence of earthquakes. The large earthquake hypothesis is problematic considering the slip rates of the faults involved when combined with the recurrence intervals. A 700-800 year recurrence of an earthquake rupturing the entire NIRCF would require a much higher rate than is observed, as displacement per event would be larger based on scaling relationships (Wells and Coppersmith, 1994; Leonard, 2010). In contrast, similar patterns of sequential ruptures have been observed on continental strike-slip faults around the world, including the North Anatolian fault of Turkey (Stein et al., 1997; Rockwell, 2011) and the Velino-Magnola fault of central Italy (Schlagenhauf et al., 2011).

The apparent temporal pattern in earthquake occurrence (figure 12) raises important questions regarding the spatial extent of earthquake ruptures on the NIRC fault system. Models of static Coulomb stress change on the offshore faults of the NIRC system found a ~30-40% likelihood for a full-length rupture of those segments (Sahakian et al., 2017). The most beneficial situation that would promote a through-going rupture of the offshore segments is one in which rupture is initiated on the Carlsbad segment, which would result in a southward-directed rupture into San Diego (Sahakian et al., 2017). Several geomorphic indicators of reversed polarity effects associated with unidirectional ruptures in San Diego indicate that the RCF may experience unidirectional southward-directed ruptures (Ben-Zion et al., 2012; Sahakian et al., 2017). However, high resolution CHIRP seismic data on the offshore NIRC segments reveal that the subsurface depth of deformation, and therefore recency of faulting, is variable along strike with the most recent faulting seen at the southern and northern ends of the offshore segments (Klotsko et al., 2015; Sahakian et al., 2017). While the possibility exists that if those offshore segments with a lack of deformation experience pure horizontal displacement it

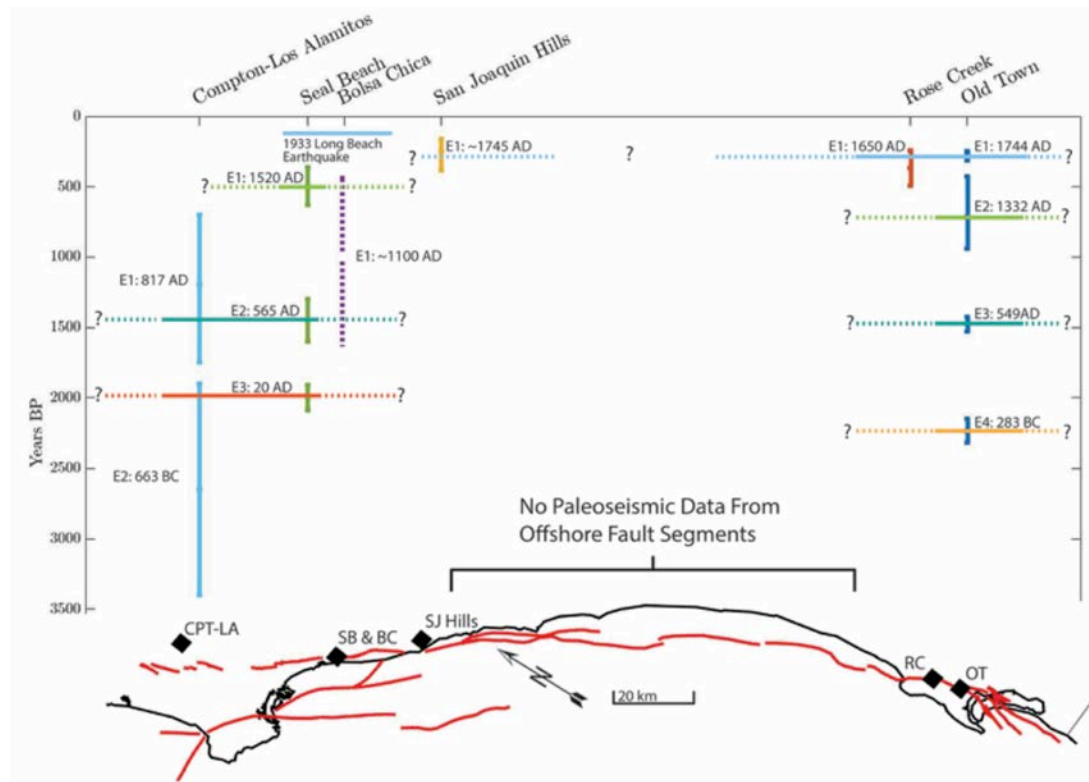


Figure 12. Earthquake occurrence along the NIRC Fault System, which shows the reported occurrence of earthquakes at several paleoseismic sites along strike of the NIRC system. Map at bottom shows trace of the NIRC fault in red, as well as locations of paleoseismic sites (black squares). For the Old Town site only those events interpreted to be of larger magnitude ($\sim M > 6.5$) are shown. Paleoseismic data from Grant et al., (1997), Grant et al. (2002), Leon et al., (2009), Leeper et al., (2017), Rockwell and Murbach (1996).

may be below the resolution of CHIRP imaging, the offshore segments appear to have not experienced an end to end rupture during the late Holocene (Klotsko et al., 2015; Sahakian et al., 2017), consistent with a sequential rupture model rather than the “wall-to-

wall” rupture inferred to be possible by Sahakian et al. (2017). Therefore, our preferred interpretation is one where the southern portion of NIRC; made up of the onshore RCF from San Diego Bay to offshore La Jolla, and possibly the Torrey Pines segment of Sahakian et al., (2017), rupture together in moderately large earthquakes. North of the Carlsbad segment, which apparently has not ruptured to the surface in the past ~ 8,000 years and may act as a barrier to through going ruptures, the Camp Pendleton strands and the onshore NI segments from at least Newport Beach to the Compton area, may rupture together (Sahakian et al., 2017; Klotsko et al. 2015).

The lack of large magnitude earthquakes in the paleoseismic record for the northernmost segments of the NIRC fault suggest that these segments may be closer to failure (Figure 12). Indeed, the northern NI fault zone has previously been identified as a possible seismic gap, with no known date for a last rupture (Grant and Rockwell, 2002; Byrant, 1988). Historical seismicity, such as the 1933 Long Beach earthquake and several smaller, deeper events beneath the oil fields north of Long Beach, confirm that these strands are active (Hauksson and Gross, 1991; Topozada et al., 1989). However, it may also be the case that the northernmost segments of the NIRC behave in a similar fashion to the Carlsbad segment offshore, perhaps rupturing only in rare events.

Conclusions

The results from our paleoseismic study at Old Town show that the Rose Canyon Fault has sustained seismic activity with ground rupturing earthquakes throughout the late Holocene and into the Historical period. The last relatively larger magnitude earthquake on the Rose Canyon Fault at Old Town was apparently sometime in the mid-18th century likely just prior to Spanish arrival in California. Additionally, the Old Town site contained evidence for a historical rupture on the Rose Canyon Fault, which records suggest is the May 27th 1862 earthquake. Furthermore, these results suggest that the Rose Canyon Fault has a ~700-800 year recurrence interval for relatively larger magnitude earthquake (M 6.7-7) that likely rupture the entire onshore portion of the Rose Canyon Fault in San Diego. This recurrence interval is several hundred years shorter than previous estimates and suggests a smaller slip per event as discussed above. The close correlation in time of dated earthquakes at paleoseismic sites along strike of the Newport-Inglewood-Rose Canyon fault system suggest that the various fault segments communicate stress in either very large magnitude earthquakes or a cascading sequence of earthquakes. Given the low reported slip rates of the faults involved, the relatively short ~700-800 year recurrence interval, as well as the apparently lack of deformation on some of the offshore fault segments our preferred interpretation is one which favors a cascading sequence of earthquakes along the Newport-Inglewood-Rose Canyon fault system.

Data and Resources

Paleoearthquakes dates presented in this paper have been taken from published works listed in the reference section below. Active fault traces in this paper are from the USGS Fold and Faults Database of the U.S. Geological Survey (<http://earthquake.usgs.gov/hazards/qfaults/>). Some plots were made using Generic Mapping Tools (GMT) version 5.4.3 (Wessel et al., 2013). Coastal Relief model acquired from the National Geophysical Database (National Geophysical Data Center, 2003)

Radiocarbon dates were calibrated and age model constructed by OxCal v4.3.2. (Bronk Ramsey, 2009)

References

- Abbott, P. L. 1991. "Flood Control in the Lower Reaches of the San Diego River." In *Environmental Perils, San Diego Region*, edited by Patrick Abbott and William Elliott, 189–94. San Diego, CA: San Diego Association of Geologist for the Geological Society of America Annual Meeting.
- Agnew, D. C., M. Legg, and C. Strand. 1979. "Earthquake History of San Diego." In *Earthquake and Other Perils: San Diego Region*, edited by Patrick L. Abbott and WJ. Elliott, 123–38. San Deigo, CA: San Diego Association of Geologist.
- Anderson, J G., T. K. Rockwell, and D. C. Agnew. 1989. "Past and Possible Future Earthquakes of Significance to the San Diego Region." *Earthquake Spectra* 5 (2): 299–335.
- Ben-Zion, Y., T. K. Rockwell, Z. Shi, and S. Xu. 2012. "Reversed-Polarity Secondary Deformation Structures Near Fault Stepovers." *Journal of Applied Mechanics* 79 (3): 031025. <https://doi.org/10.1115/1.4006154>.
- Biasi, G. P., R. J. Weldon, T. E. Fumal, and G. G. Seitz. 2002. "Paleoseismic Event Dating and the Conditional Probability of Large Earthquakes on the Southern San Andreas Fault, California." *Bulletin of the Seismological Society of America* 92 (7): 2761–81. <https://doi.org/10.1785/0120000605>.
- Bronk Ramsey, C. 2009. "Bayesian Analysis of Radiocarbon Dates." *Radiocarbon* 51 (1): 337–60.
- Byrant, W. A. 1988. "Recently Active Traces of the Newport-Inglewood Fault Zone, Los Angeles and Orange Counties, California." Sacramento. <https://doi.org/DMG OFR 88-14>.
- Demere, T. A. 1982. "Review of the Lithostratigraphy, Biostratigraphy and Age Of the San Diego Formation." In *Geologic Studies in San Diego I*, edited by Patrick L. Abbott, 127–34. San Deigo, CA: San Diego Association of Geologist.
- Elders, W. A., R. W. Rex, P. T. Robinson, S. Biehler, and T. Meidav. 1972. "Crustal Spreading in Southern California." *Science* 178 (4056): 15–24.
- Fuis, G. S. 1982. "Displacement on the Superstition Hills Fault Triggered by the Earthquake." *USGS Report: The Imperial Valley, California, Earthquake of October 15, 1979*.
- Grant, L. B., L. J. Ballenger, and E. E. Runnerstrom. 2002. "Coastal Uplift of the San Joaquin Hills, Southern Los Angeles Basin, California, by a Large Earthquake since A.D. 1635." *Bulletin of the Seismological Society of America* 92 (2): 590–99. <https://doi.org/10.1785/0120010119>.
- Grant, L. B., J. T. Waggoner, T. K. Rockwell, and C. Von Stein. 1997. "Paleoseismicity of the North Branch of the Newport-Inglewood Fault Zone in Huntington Beach, California, from Cone Penetrometer Test Data." *Bulletin of the Seismological Society of America* 87 (2): 277–93.
- Grant, L. B., and T. K. Rockwell. 2002. "A Northward-Propagating Earthquake Sequence in Coastal Southern California." *Seismological Research Letters* 73 (4): 461–69.
- Hauksson, E., and S. Gross. 1991. "Source Parameters of the 1933 Long-Beach Earthquake." *Bulletin of the Seismological Society of America* 81 (1): 81–98.

- Heusser, L. 1978. "Pollen in Santa Barbara Basin, California: A 12,000-Yr Record." *Geological Society of American Bulletin* 89: 673–78.
- Kennedy, M. P. 1975. "Geology of the San Diego Metropolitan Area, California." *California Division of Mines and Geology Bulletin* 200: 9–39.
- Kennedy, M.P. and E.E. Welday. 1980. Recency and character of faulting offshore metropolitan San Diego, California. *Calif. Div. Mines and Geol. Map Sheet* 40.
- Kennedy M.P. and S.H. Clarke. 1999. Age of faulting in San Diego Bay in the vicinity of the Coronado Bridge; Addendum to analysis of late Quaternary faulting in San Diego Bay and hazard to Coronado Bridge. *Calif. Div. Mines and Geol., Open File Report* 97-10B, 12 p plus seismic lines.
- Kern, J. P., and T. K. Rockwell. 1992. "Chronology and Deformation of Quaternary Marine Shorelines, San Diego County, California." *Quaternary Coasts of the United States*, no. 48: 377–82.
- Kies, R. P. 1982. "Paleogeography of the Mt. Soledad Formation West of the Rose Canyon Fault." In *Geologic Studies in San Diego*, edited by Patrick L. Abbott, 1–11. San Diego, CA: San Diego Association of Geologist.
- Klotsko, S., N. Driscoll, G. Kent, and D. Brothers. 2015. "Continental Shelf Morphology and Stratigraphy Offshore San Onofre, California: The Interplay between Rates of Eustatic Change and Sediment Supply." *Marine Geology* 369. Elsevier B.V.: 116–26. <https://doi.org/10.1016/j.margeo.2015.08.003>.
- Leeper, R., B. Rhodes, M. Kirby, K. Scharer, J. Carlin, E. Hemphill-Haley, S. Avnaim-Katav, G. Macdonald, S. Starratt, and A. Aranda. 2017. "Evidence for Coseismic Subsidence Events in a Southern California Coastal Saltmarsh." *Scientific Reports* 7 (March). Nature Publishing Group: 1–11. <https://doi.org/10.1038/srep44615>.
- Legg, M., and D. C. Agnew. 1979. "The 1862 Earthquake in San Diego." In *Earthquake and Other Perils: San Diego Region*, edited by Patrick L. Abbott and W.J. Elliot, 139–41. San Deigo, CA: San Diego Association of Geologist.
- Leon, L. A., J. F. Dolan, J. H. Shaw, and T. L. Pratt. 2009. "Evidence for Large Holocene Earthquakes on the Compton Thrust Fault, Los Angeles, California." *Journal of Geophysical Research: Solid Earth* 114 (12): 1–14. <https://doi.org/10.1029/2008JB006129>.
- Leonard, M. 2010. "Earthquake Fault Scaling: Self-Consistent Relating of Rupture Length, Width, Average Displacement, and Moment Release." *Bulletin of the Seismological Society of America* 100 (5 A): 1971–88. <https://doi.org/10.1785/0120090189>.
- Lindvall, S., and T. K. Rockwell. 1995. "Holocene Activity of the Rose Canyon Fault Zone in San Diego, California." *Journal of Geophysical Research* 100 (B12): 24121–32.
- Moore, G. W. 1972. "Offshore Extension of the Rose Canyon Fault, San Diego, California." *Geological Survey Professional Paper* 800–2: 113–16.
- Moore, G. W., and M. P. Kennedy. 1975. "Quaternary Faults at San Diego Bay, California." *J. Res. US Geol. Surv.* Vol. 3.
- National Geophysical Data Center, 2003. U.S. Coastal Relief Model - Southern California. National Geophysical Data Center, NOAA. doi:10.7289/V500001J [April 17, 2018].
- Nielsen, S. B., and L. Knopoff., 1998. "The Equivalent Strength of Geometrical Barriers

- to Earthquakes.” *Journal of Geophysical Research* 103 (B5): 9953–65.
- Reimer, P. J., E. Bard, A. Bayliss, J. W. Beck, G. P. Blackwell, and C. Bronk Ramsey. 2013. “Intcal13 and Marine13 Radiocarbon Age Calibration Curves 0–50,000 Years Cal Bp.” *Radiocarbon* 55 (4): 1869–87.
www.radiocarbon.org.%0Awww.radiocarbon.org.
- Rockwell, T. K. 2010a. “The Rose Canyon Fault Zone in San Diego.” *Fifth International Conference on Recent Advances in Geotechnical Earthquake Engineering and Soil Dynamics and Symposium in Honor of Professor I.M. Idriss*, no. 7.06c: 1–9.
- Rockwell, T. K. 2010b. “Seismic Source Characteristics of Onshore Rose Canyon Fault.” *San Onofre Nuclear Generating Station Seismic Hazard Assessment Program 2010 Seismic Hazard Analysis Report; Appendix A, Attachment A-2*.
- Rockwell, T. K. 2011. “The North Anatolian Fault.” In *Encyclopedia of Natural Hazards*, edited by Peter T. Bobrowsky. Springer Science+Business Media.
<https://doi.org/10.1007/978-1-4020-4399-4>.
- Rockwell, T. K., S. Lindvall, C. C. Haraden, K. C. Hirabayashi, and E. Baker. 1991. “Minimum Holocene Slip Rate for the Rose Canyon Fault in San Diego, California.” In *Environmental Perils: San Diego Region*, edited by Patrick L. Abbott and William J. Elliott, 37–46. San Diego, CA: San Diego Association of Geologists for the Geological Society of America Annual Meeting.
- Rockwell, T. K., and M. Murbach. 1999. “Holocene Earthquake History of the Rose Canyon Fault Zone.” U.S. Geological Survey Final Technical Report for Grant No. 1434-95-26133
- Rockwell, T. K., K. M. Scharer, and T. E. Dawson. 2016. Earthquake Geology and Paleoseismology of Major Strands of the San Andreas Fault System: Chapter 38. *Applied Geology in California* 26: 721–56.
<http://pubs.er.usgs.gov/publication/70177065>.
- Sahakian, V., J. Bormann, N. Driscoll, A. Harding, G. Kent, and S. Wesnousky. 2017. “Seismic Constraints on the Architecture of the Newport-Inglewood/Rose Canyon Fault: Implications for the Length and Magnitude of Future Earthquake Ruptures.” *Journal of Geophysical Research: Solid Earth* 122 (3): 2085–2105.
<https://doi.org/10.1002/2016JB013467>.
- Schlagenhauf, A., I. Manighetti, L. Benedetti, Y. Gaudemer, R. Finkel, J. Malavieille, and K. Pou. 2011. “Earthquake Supercycles in Central Italy, Inferred From ³⁶Cl Exposure Dating.” *Earth and Planetary Science Letters* 307 (3–4). Elsevier B.V.: 487–500. <https://doi.org/10.1016/j.epsl.2011.05.022>.
- Rugg, S., R. Torres, and T. K. Rockwell. 2013. “TDY Fault Study: San Diego International Airport.” Kleinfelder Final Report for the San Diego County Regional Airport Authority, San Diego, CA, Kleinfelder Project No. 125800.
- Stein, R. S., A. A. Barka, and J. H. Dieterich. 1997. “Progressive Failure of the North Anatolian Fault since 1939 by Earthquake Stress Triggering.” *Geophysical Journal International* 128: 594–604.
- Stein, R. S., G. C. P. King, and J. Lin. 1992. “Change in Failure Stress on the Southern San Andreas Fault System Caused by the 1992 Magnitude = 7.4 Landers Earthquake.” *Science* 258 (5086): 1328–32.
- The Los Angeles Star*. June 21, 1862. “San Diego Items-Earthquakes,” p.2 col. 2.
- Topozada, T., J. H. Bennett, G. Borchardt, R. Saul, and J. F. Davis. 1989. “Earthquake

- Planning Scenario for a Major Earthquake on the Newport-Inglewood Fault Zone.” *Division of Mines and Geology: California Geology* 42 (4).
- Vendrasco, M. J., Eernisse, D. J., Powell, C. L., II, and Fernandez, C. Z. 2012. Polyplacophora (Mollusca) from the San Diego Formation: A remarkable assemblage of fossil chitons from the Pliocene of southern California. *Natural History Museum of Los Angeles County, Contributions in Science*, no. 520: 15-72, figs. 1-22, tables 1-2.
- Wei, M., D. Sandwell, Y. Fialko, and R. Bilham. 2011. “Slip on Faults in the Imperial Valley Triggered by the 4 April 2010 Mw 7.2 El Mayor-Cucapah Earthquake Revealed by InSAR.” *Geophysical Research Letters* 38 (1): 1–6. <https://doi.org/10.1029/2010GL045235>.
- Wells, D. L., and K. J. Coppersmith. 1994. “New Empirical Relationships among Magnitude, Rupture Length, Rupture Width, Rupture Area, and Surface Displacement.” *Bulletin of the Seismological Society of America* 84 (4): 974–1002. <https://doi.org/10.1029/1993bs01731>.
- Wessel, P., W. H. F. Smith, R. Scharroo, J. F. Luis, and F. Wobbe, Generic Mapping Tools: Improved version released, *EOS Trans. AGU*, 94, 409-410, 2013
- Woodward and Clyde. 1985. Geologic and fault investigation, San Diego police administration and technical center, San Diego, CA. Technical report for Starboard Development Company,
- Woodward and Clyde. 1994. Report of fault hazard investigation for the entertainment and sports center, San Diego, California. Geotechnical report for Centre City Development Corporation.
- Wright, T. L. 1991. “Structural Geology and Tectonic Evolution of the Los Angeles Basin, California.” In *Active Margin Basins*, edited by Kevin T. Biddle, AAPG Memoir, 35–79. Tulsa, OK: The American Association of Petroleum Geologist.